A study of the cluster effect on fatigue crack initiation

Yoann Guilhem, Georges Cailletaud, Stéphanie Basseville, Francois Curtit, Jean-Michel Stephan

A study of the cluster effect on fatigue crack initiation

Y. Guilhem[1,3], *G. Cailletaud*[1], *S. Basseville*[2], *F. Curtit*[3], *J.M Stéphan*[3]
[1]*Centre des Matériaux, Mines-ParisTech, CNRS UMR7633, 91003 Evry cedex, France;*
[2]*LISV, Université de Versailles, Versailles, France;*
[3]*EDF R&D, Moret-sur-Loing, France*

1 Introduction

Fatigue crack initiation is classically predicted by macroscopic models, where the critical variables are combinations of macroscopic stress and strain. Nevertheless, the local mechanisms responsible for crack initiation in metals and alloys are persistent slip bands (PSB), which develop on a microscale, in each grain. Having in view a better understanding of the local mechanisms, the purpose of this work is to get an improved knowledge of the local stress and strain fields and to examine the result obtained by using the relevant variables in local crack initiation models.

The various regimes associated to crack propagation were characterized a long time ago (see for instance [1]). Stage I (initiation) and stage II (propagation) were introduced. During the initiation period, cracks are small enough to directly interact with the microstructure. Since they are related to PSB's, their direction is governed by crystal plasticity and follow slip planes containing slip systems with a maximum Schmid factor in the first surface grain. The propagation rate is then affected by the local geometry, and cannot be predicted by linear elastic fracture mechanics using global variables [2, 3]. The key point is that the size of the plastic zone generated by the crack is smaller than the plastic zone associated with the microstructure effect. The competition between the microcracks and the local microstructure explains the threshold concept: the macroscopic threshold can be seen as the macroscopic stress value for which short cracks will initiate but stop.

After initiation in PSB, small cracks tend to propagate in shear mode until they reach grain boundaries where the growth rate decreases significantly. It has been shown that this retardation is due to the crystallographic misorientation between the adjacent grains that generates slip incompatibilities at the boundaries [4]. The parameters like crystal orientation, grain size and shape have then to be taken into account to reproduce local strain heterogeneities which govern crack initiation. Having in hand all these observations (see also for instance [5, 6]), it is now useful to complement the experimental data by relevant numerical investigations.

Having a full simulation of a real 3D microstructure with hundreds of grains including a real crack with a fine mesh loaded for several thousands of cycles is still out of reach, this is why authors develop representative examples on reduced mi-

crostructures. Two dimensional ruled meshes are used for instance on single crystal, bicrystals [7] and polycrystals [8]. Meshes using Voronoï tesselation, but also two-dimensional meshes are introduced to investigate the propagation of a microcrack [9]. Using a crystal plasticity model, it was shown that the crack propagation was directed by two primary slip planes. The crack tip opening exhibits large changes due to the orientation of the grains in the vicinity [10]. It is also shown that cracks will preferably initiate from the "soft" grains [11]. So, the investigations are more directed toward the orientation of each grain, or to grain boundary misorientation.

The aim of this work is to introduce a new element in the discussion, pointing out the fact that stress redistribution operates on grain clusters more than on individual grains or just couples of grains. Finite elements are then used to study the effect of particular grains "clusters" located at the free surface of the aggregate and to show how the different grains interact to each other. A statistical study is performed to characterize the influence of the surrounding on soft or hard grains, oriented for easy slip or not. The multiaxial state of stress will be studied. A crystal plasticity model with nonlinear kinematic hardening is introduced in a regular 2D mesh which conforms grain boundaries. The results on a microscale are finally used in a classical fatigue life prediction model to predict local crack initiation.

2 Description of the numerical model

2.1 Crystal plasticity model

A crystal plasticity model available in the Finite Element code ZeBuLoN [12] is used. Small strain assumption is used, since cyclic loading produces limited strains. Each grain is considered as a single crystal and the strain fields are supposed to be continuous at grain boundaries. Stress discontinuities can then appear in these sites. The partition of the strain rate tensor introduces an elastic and a viscoplastic part:

$$\dot{\underset{\sim}{\varepsilon}} = \dot{\underset{\sim}{\varepsilon}}^e + \dot{\underset{\sim}{\varepsilon}}^p = \underset{\approx}{C}^{-1} : \dot{\underset{\sim}{\sigma}} + \dot{\underset{\sim}{\varepsilon}}^p \tag{1}$$

Cubic elasticity is defined by the fourth order stiffness tensor $\underset{\approx}{C}$, so that elasticity itself is the source of residual intergranular stresses. The resolved shear stress τ^s is computed on slip system s by means of the orientation tensor $\underset{\sim}{\boldsymbol{m}}^s$:

$$\tau^s = \underset{\sim}{\boldsymbol{\sigma}} : \underset{\sim}{\boldsymbol{m}}^s \quad \text{with} \quad \underset{\sim}{\boldsymbol{m}}^s = \frac{1}{2}\left(\underline{\boldsymbol{l}}^s \otimes \underline{\boldsymbol{n}}^s + \underline{\boldsymbol{n}}^s \otimes \underline{\boldsymbol{l}}^s\right) \tag{2}$$

Here, $\underline{\boldsymbol{n}}^s$ is the normal to the slip plane, and $\underline{\boldsymbol{l}}^s$ is the slip direction. The viscoplastic slip rate $\dot{\gamma}^s$ is given by a power function of the resolved shear stress, then the viscoplastic strain rate tensor is defined as the sum of the contributions of all the slip systems.

$$\dot{v}^s = \left\langle \frac{|\tau^s - x^s| - R_0 - r^s}{K} \right\rangle^n \quad \dot{\gamma}^s = \dot{v}^s \text{sign}\left(\tau^s - x^s\right) \quad \dot{\underset{\sim}{\varepsilon}}^p = \sum_s \dot{\gamma}^s \underset{\sim}{\boldsymbol{m}}^s \tag{3}$$

where K and n are the parameters which define viscosity, R_0 the initial resolved shear stress, and where x^s and r^s are respectively the kinematic hardening and the isotropic hardening variables. These variables depend on two state variables, namely α^s and ρ^s:

$$x^s = c\alpha^s \tag{4}$$

$$r^s = bQ \sum_r h_{sr}\rho^r \tag{5}$$

$$\dot{\alpha}^s = \big(sign(\tau^s - x^s) - d\alpha^s\big)\dot{v}^s \tag{6}$$

$$\dot{\rho}^s = \big(1 - b\rho^s\big)\dot{v}^s \tag{7}$$

The material parameters are c, d (kinematic hardening), Q, b (isotropic hardening). The interaction matrix h_{sr} introduces self-hardening (diagonal terms) and latent hardening between the different slip systems. All the values used for the FE simulation are listed in Fig. 1(d).

Since the paper is restricted to a numerical study, it was decided to perform 2D computations only. A generalized plane strain assumption is used, and only one active slip system is allowed in each grain. The vectors $\underline{\boldsymbol{n}}$ and $\underline{\boldsymbol{l}}$ are both located in the plane (x_1,x_2), and θ is the angle between x_1 and the slip direction, so that:

$$\underline{\boldsymbol{l}}^T = (\cos\theta \ \ \sin\theta \ 0) \qquad \underline{\boldsymbol{n}}^T = (-\sin\theta \ \ \cos\theta \ 0) \tag{8}$$

According to this notation, a grain is called "hard" for $\theta = 0°$ (zero resolved shear stress if computed with the macroscopic stress tensor) and "soft" for $\theta = 45°$ (maximum resolved shear stress if computed with the macroscopic stress tensor).

The accumulated viscoplastic strain rate p and its related average in a grain (volume V_g) $\langle p\rangle^g$, which are regarded as primary variables are written as:

$$p = \int_0^t \dot{v}\, dt \qquad \langle p\rangle^g = \frac{1}{V_g}\int_{V_g} p\, dV \tag{9}$$

2.2 Finite elements mesh, boundary conditions

The mesh consists of a 71 grain polycrystalline aggregate composed of 10561 nodes and 5178 generalized plane strain elements with a quadratic interpolation. All grains have an regular hexagonal shape, so that there is no trouble produced by a variable shape or size. As shown in Fig. 1, the grains at the boundaries can be "open" (an hexagon is cut by the surface) or "closed" (a full hexagon touches the surface). The differences between these two types of grains will be investigated later.

Symmetry conditions are applied at the bottom ($u_2 = 0$) and the right side ($u_1 = 0$) of the mesh, as displayed in Fig. 1(a). A cyclic loading of $\pm 2\%$ average strain is applied on the top of the aggregate for 10 cycles. The left edge is a free surface.

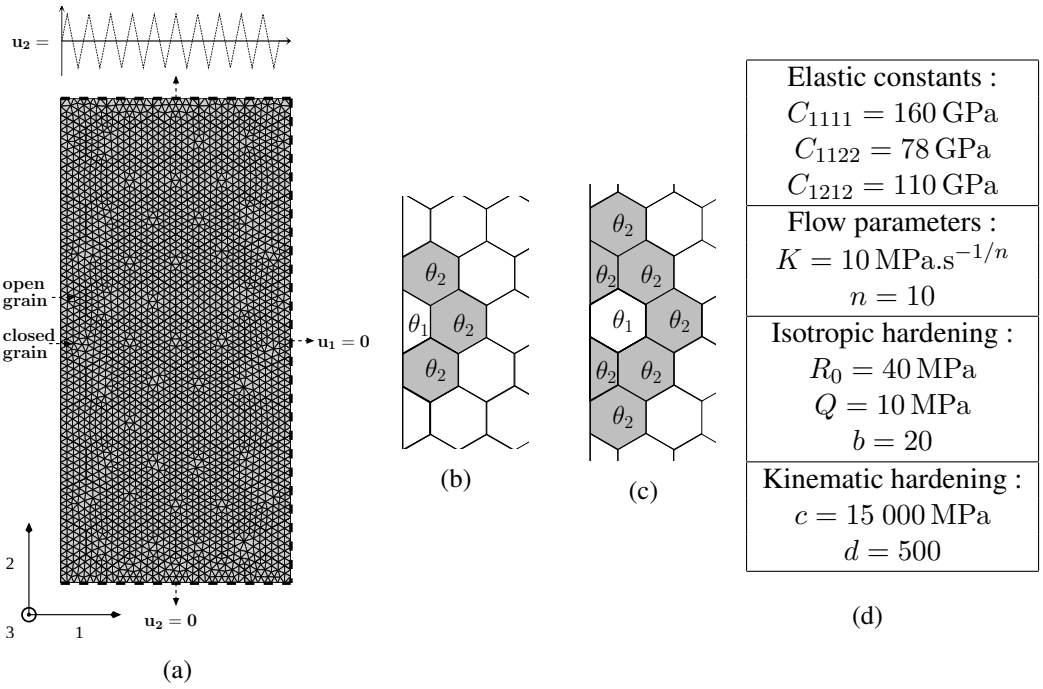

Fig. 1: Definition of the various Finite Element calculations: (a) mesh and boundary conditions; (b) Configuration of a surface cluster centered on an open grain; (c) configuration of a surface cluster centered on a closed grain; (d) material parameters

3 Results and discussion

Two types of computation have been performed, under symmetric prescribed strain and an amplitude of 2%. All the grains of the aggregate are randomly oriented, but a few of them near the surface have a specific arrangement in order to create "clusters". A series of extreme situations have then been created, in order to exhibit the effect of soft or hard clusters and to generate extreme situations for the local stress fields. In each case, a large number of calculations have been performed, in order to make a statistical treatment of the results.

3.1 Random aggregates

First, 800 computations with different orientation sets were performed. The average cumulated shear strain is shown in Fig. 2 as a function of the grain orientation. The result that would be obtained with a single crystal is also plotted as a reference. The difference between the two illustrates the "structure" effect produced by neighbouring grains.

The most important result is that slip is present in hard grains, that would have a zero resolved shear stress as a single crystal: due to the multiaxial stress state, the resolved shear stress is not zero on a $\theta = 0$ grain. This multiaxial effect is the consequence of local heterogeneities due to the elastic anisotropy and to the stress

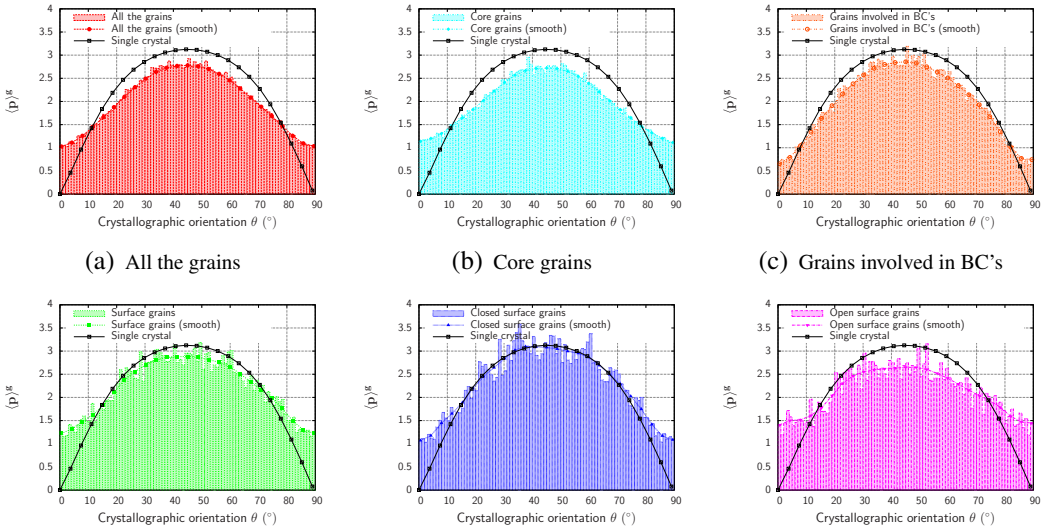

(a) All the grains (b) Core grains (c) Grains involved in BC's

(d) Surface grains (e) Closed surface grains (f) Open surface grains

Fig. 2: Plastic behavior of different types of grains and comparison with single crystal

redistribution coming from plastic flow. The opposite is true for soft grains: the amount of slip is lower in the aggregate than for the corresponding single crystal (Fig. 2(a)); this is the result of kinematic constraints that decrease plastic flow. These effects are predominant if the plot is reduced to the core grains (Fig. 2(b)). For the grains involved in boundary conditions (in contact with top, bottom or right edges) (Fig. 2(c)), they are weaker.

Concerning the surface grains, there is an important variability of the accumulated shear strain: the promotion of heterogeneity by surface is a classical result [13]. On the other hand, the amount of shear is globally higher for surface grains than for the rest of the grains, regardless of the orientation (Fig. 2(d)). Soft closed grains (Fig. 2(e)) are those which exhibit the highest cumulated shear, sometimes larger than the result given by the reference single crystal. Open grains have just a half size, and are then more influenced by the surrounding grains than by their own crystal orientation: the accumulated shear strain is partly inherited from the neighbouring grains, so that the hard open grains at the surface present the highest accumulated shear, meanwhile the soft open grains meet the level obtained for the rest of the grains (Fig. 2(f)).

3.2 Clustering effect

As previously seen, surface clusters can be created around an open grain (Fig. 1(b)) or a closed grain (Fig. 1(c)). The extreme configurations are obtained by fixing the θ_1 and θ_2 angles to get soft grains surrounded by hard ones and vice versa. Each cluster is defined by 3 parameters : the type of the central grain – open (O) or closed (C)–, the orientation of the central grain θ_1 and the orientation of the surrounding

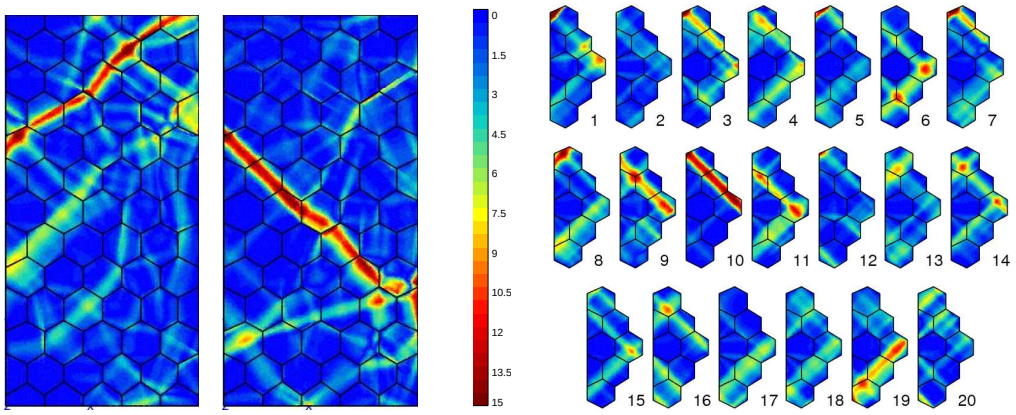

(a) (b)

Fig. 3: Contour maps of the cumulated viscoplastic shear strain for the cluster C-0-45 (different realizations): (a) whole specimen; (b) local maps on various clusters.

grains θ_2. The identification code is *type*-θ_1-θ_2. The local strain fields of many configurations were studied. The main conclusions are described by means of a few typical examples.

Figure 3 shows global and local contour maps of the accumulated shear strain p for a closed hard grain surrounded by soft ones (C-0-45). Strain localization bands are present in the specimen, following various paths according to the random set of orientations. Although the crystal orientations are the same inside the cluster, some differences appear in the strain patterns for the central grain (see for instance the local maps 1, 12 and 17 in Fig. 3(b)) and also in the surrounding grains (see local maps 2, 10 and 19 on Fig. 3(b)), depending on the orientation of the grains around the cluster.

The local stress state was also studied, in order to better understand the reason why a multiaxial effect develops. The plots still concern the central grain of the clusters (Fig. 4). The average of σ_{22} is plotted as a function of the average of σ_{11}, that is the component normal normal to the surface. Of course, this component is nil at the surface, nevertheless it increases quickly inside the grain, so that it is far from being negligible in the whole grain. Its smallest value is obtained for O-0-45 case. It is worth noting that, in the σ_{11}–σ_{22} plane, the loops can be schematized by two vertical lines (when crossing the elastic domain), and two inclined lines, the slope of which is 1 for a soft grain embedded into hard ones (C-45-0 and O-45-0), and -1 for a hard grain embedded into soft ones (C-0-45 and O-0-45). This can be explained by the elastoplastic Poisson's effect, and can be demonstrated analytically by using simplified models [14] that are not shown here for the sake of brevity.

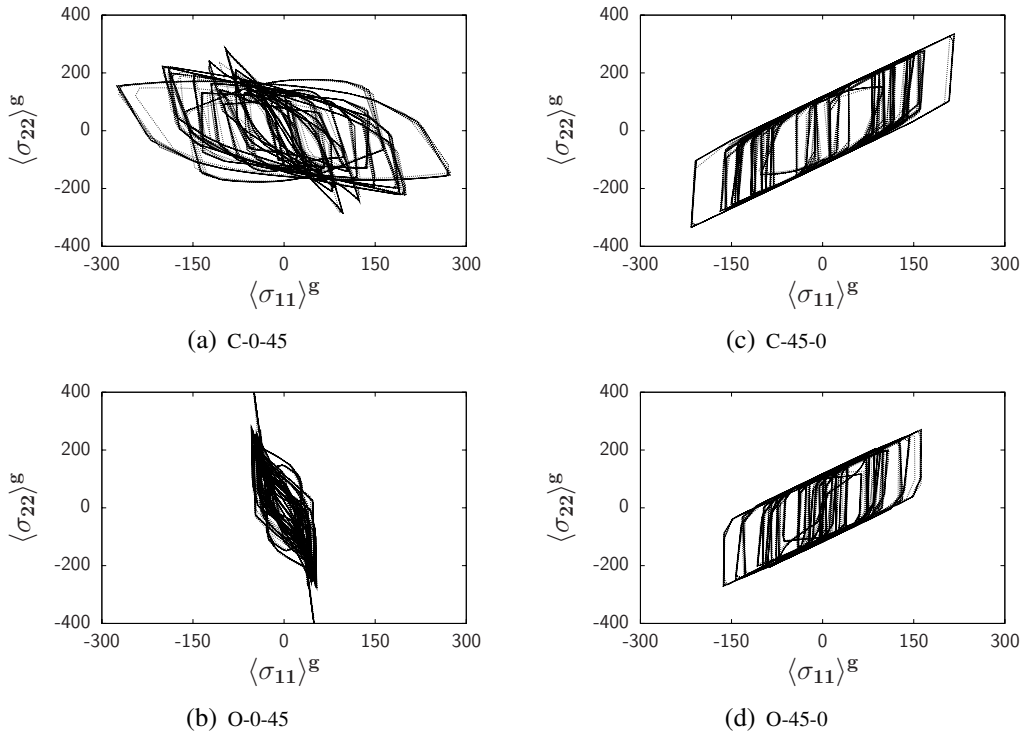

(a) C-0-45 (c) C-45-0

(b) O-0-45 (d) O-45-0

Fig. 4: Stress multiaxiality at the grain scale for different clusters

3.3 Fatigue life prediction

Dang Van's criterion is a popular model able to account for multiaxiality in fatigue life prediction [15]. It is specially devoted to the description of High Cycle Fatigue, but it is sometimes extrapolated to finite life. The idea behind the criterion is that the deviatoric component of the stress tensor is redistributed due to local plastic flow, and that crack initiation is the result of the simultaneous effect of the resulting maximum shear after redistribution combined with the hydrostatic pressure, the positive values of which will promote crack opening, and damage. In classical applications of this criterion, the input is the macroscopic stress tensor. It is adapted in the present case, where shear is considered on the slip plane instead of in the plane of maximum shear, which has no physical basis. The model simply writes:

$$\sigma_{DV} = \max_{t,s} \left(\tau_r^s(t) + bp(t)\right) \tag{10}$$

$$\tau_r^s(t) = \tau^s(t) - \frac{\tau_{min} + \tau_{max}}{2} \tag{11}$$

with $p(t)$ the current hydrostatic pressure, $\tau_r^s(t)$ the current resolved shear stress on system s after redistribution, and b a material parameter.

This criterion has been applied on randomly oriented aggregates and for various loading amplitudes (fifty different aggregates, four load levels). A classical value is used for the material parameter ($b = 0,2$). The purpose is to determine the ori-

entation (θ) of the grain where initiation occurs, together with its location (surface or interior of the aggregate). A comparison with the accumulated plastic strain rate p is shown in Fig. 5. Concerning σ_{DV}, the influence of θ is noticeable for low amplitude, but vanishes for larger ones: For an amplitude of 0.3%, the criterion value of σ_{DV} is 50% higher for soft grains than for hard grains. This ratio drops to 20% for larger amplitudes like 2%. This shows that the crystallographic effect tends to disappear in Low Cycle Fatigue (the same trend is observed about p). In addition, this criterion does not allow to naturally predict the location of the initiation. Even for low amplitudes, the largest equivalent stress is found in the core grains, and even in the grains involved in BC's. This fact disagrees with classical observations, since the core grains are predicted to fail earlier than surface grains. However, as seen in section 3.1, the accumulated plastic strain rate p is generally higher on the surface soft grains, especially in closed ones. Early initiation in the first grain is then better predicted by a model introducing accumulated plastic strain as critical variable than by a stress dependent model. A two stage criterion based on p for the initation, followed by stress for the subsequent propagation in the next grains would be more consistent with the experimental observations.

4 Concluding remarks

Using data from the microscale is a promising direction to improve damage and fatigue crack initiation models. The crystalline level seems to be appropriate, since slip plays an important role in crack initiation. The easy way is then to introduce crystal orientation and to determine a criterion taking into account the local orientation of each grain only. The present paper demonstrates that the kinematic constraints in the aggregates introduce a microstructure effect, and that a good microstructural model must take into account the grain, together with its surrounding. The cluster effect characterized in the paper produces a strong multiaxiality, even for onedimensional macroscopic load. It enhances local slip in grains that have a very low macroscopic Schmid factor. It was shown that crystallographic orientation has stronger influence at low amplitude loadings than at high ones. The need of a two components criterion was also demonstrated to predict inititation and propagation in adequation with experimental studies.

References

[1] K. J. Miller, The behaviour of short fatigue cracks and their initiation. Part II– A General summary, Fatigue and Fracture of Engng Mat and Struct 10 (1987) 93–113.

[2] S. Pearson, Initiation of fatigue cracks in commercial aluminium alloys and the subsequent propagation of very short cracks, Engng Fracture Mechanics 7 (1975) 235–247.

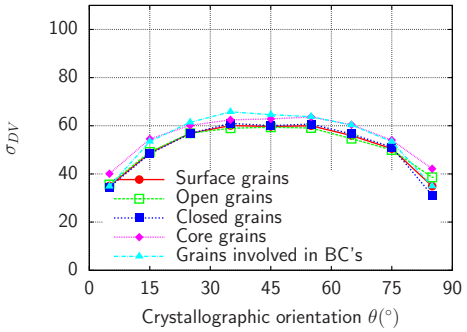

(a) $\Delta/2E = 0.3\%$

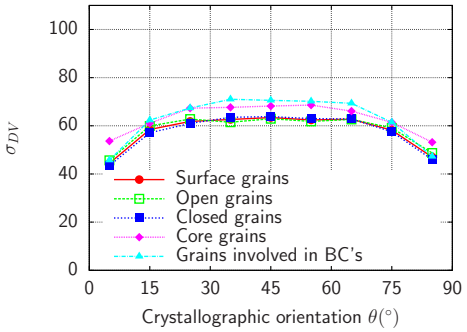

(b) $\Delta/2E = 0.5\%$

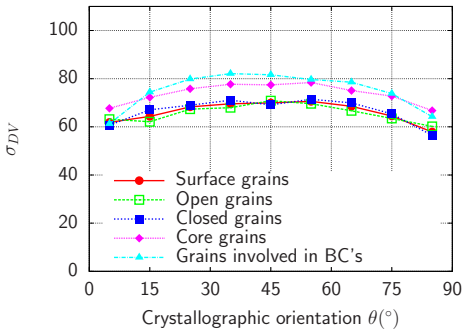

(c) $\Delta/2E = 1.0\%$

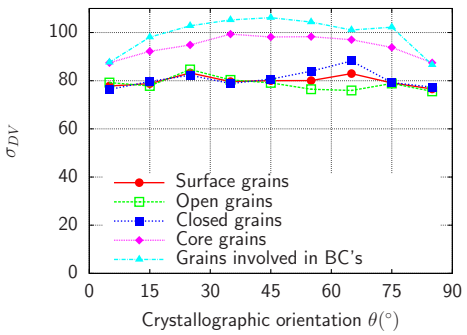

(d) $\Delta/2E = 2.0\%$

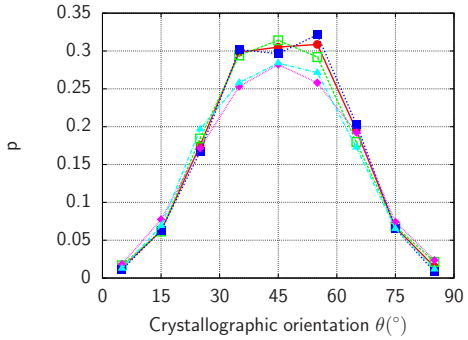

(e) $\Delta/2E = 0.3\%$

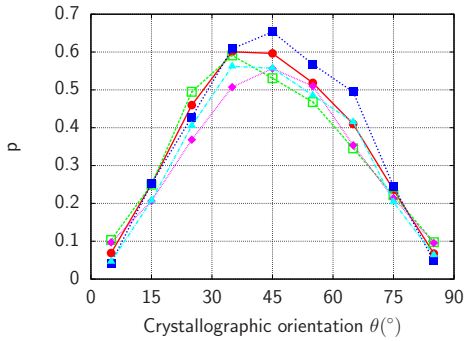

(f) $\Delta/2E = 0.5\%$

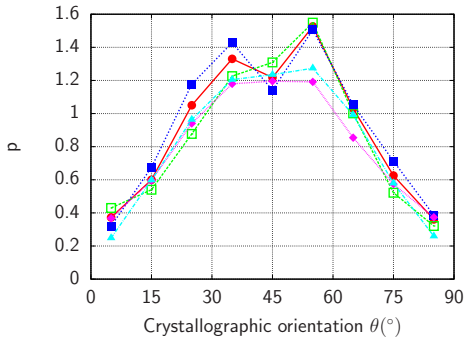

(g) $\Delta/2E = 1.0\%$

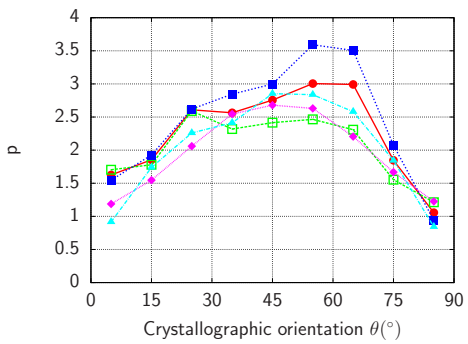

(h) $\Delta/2E = 2.0\%$

Fig. 5: Dang Van criterion and accumulated plastic strain rate related to crystallographic orientation for different loading amplitudes (grain average values)

[3] K. J. Miller, The short crack problem, Fatigue and Fracture of Engng Mat and Struct 5 (1982) 223–232.

[4] T. H. Lin, K. K. F. Wong, N. J. Teng, S. R. Lin, Micromechanic analysis of fatigue band crossing grain boundary, Material Science and Engineering A 246 (1998) 169–179.

[5] E. Sackett, L. Germain, M. Bache, Crystal plasticity, fatigue crack initiation and fatigue performance of advanced titanium alloys, Int. J. Frac 29 (2007) 2015–2021.

[6] X.-L. Wang, Y. Wang, A. Stoica, D. Horton, H. Tian, P. Liaw, H. Choo, J. Richardson, E. Maxey, Inter- and intragranular stresses in cyclically-deformed 316 stainless steel, Material Science and Engineering A 399 (2005) 114–119.

[7] G. P. Potirniche, S. R. Daniewicz, Finite element modeling of microstructurally small cracks using single crystal plasticity, Int. J. Fatigue 25 (2003) 877–884.

[8] V. P. Bennett, D. L. McDowell, Polycrystal orientation distribution effects on microslip in high cycle fatigue, Int. J. Fatigue 25 (2003) 27–39.

[9] I. Simonovski, L. Cizelj, The influence of grain's crystallographic orientations on advancing short crack, Int. J. Fatigue 29 (2007) 2005–2014.

[10] I. Simonovski, K. F. Nilsson, L. Cizelj, Crack tip displacement of microstructurally small cracks in 316L steel and their dependence on crystallographic orientations of grains, Fatigue and Fracture of Engng Mat and Struct 30 (2007) 463–478.

[11] K.-S. Cheong, M. Smillie, D. Knowles, Predicting fatigue crack initiation through image-based micromechanical modeling, Acta Mat. 55 (2007) 1757–1768.

[12] L. Méric, G. Cailletaud, Single crystal modeling for structural calculations. Part 2: Finite element implementation, J. of Engng. Mat. Technol. 113 (1991) 171–182.

[13] F. Barbe, S. Forest, G. Cailletaud, Intergranular and intragranular behavior of polycrystalline aggregates. Part II: Results, Int. J. of Plasticity 17 (4) (2001) 537–566.

[14] Y. Guilhem, S. Basseville, F. Curtit, J.-M. Stéphan, G. Cailletaud, Investigation of the effect of grain clusters on fatigue crack initiation in polycrystals, International Journal of Fatigue (submitted).

[15] K. Dang Van, Sur la résistance à la fatigue des métaux, Sciences et techniques de l'armement 47 (1973) 647–722.